Inner-mitochondrial membrane protein PfMPV17 is linked to P. falciparum in vitro resistance to the indoloquinolizidine alkaloid alstonine

Author

Macdonald, JR, Arnold, MS, Luth, MR, Cihalova, D, Quinn, RJ, Winzeler, EA, Lee, MC, van Dooren, GG, Maier, AG, Skinner-Adams, TS, Andrews, KT, Fisher, GM

Published

2025

Journal Title

Journal of Antimicrobial Chemotherapy

Version

Version of Record (VoR)

DOI

10.1093/jac/dkaf141

J Antimicrob Chemother 2025; **80**: 1869–1877
https://doi.org/10.1093/jac/dkaf141 Advance Access publication 28 May 2025

Journal of Antimicrobial Chemotherapy 50 years

Inner-mitochondrial membrane protein *Pf*MPV17 is linked to *P. falciparum in vitro* resistance to the indoloquinolizidine alkaloid alstonine

J. R. Macdonald[1], M. S. Arnold[1], M. R. Luth[2], D. Cihalova[3], R. J. Quinn[1], E. A. Winzeler[4], M. C. Lee[5], G. G. van Dooren[3], A. G. Maier[3], T. S. Skinner-Adams[1], K. T. Andrews[1]*† and G. M. Fisher[1]†

[1]Institute for Biomedicine and Glycomics, Griffith University, Brisbane, Queensland, Australia; [2]Department of Pediatrics, University of California, San Diego, USA; [3]Research School of Biology, Australian National University, Canberra, ACT, Australia; [4]Department of Pediatrics, School of Medicine, and Skaggs School of Pharmacy and Pharmaceutical Sciences, University of California, San Diego, USA; [5]Division of Biological Chemistry and Drug Discovery, University of Dundee, Dundee DD1 5EH, UK

*Corresponding author. E-mail: k.andrews@griffith.edu.au
†Co-senior authors.

Received 29 September 2024; accepted 27 April 2025

Background: There are an estimated 260 million malaria cases and ~600 000 deaths annually. Challenges to malaria eradication include the lack of highly effective and broadly applicable vaccines and parasite drug resistance. This is driving the need for new tools, including novel drugs and drug targets. The indoloquinolizidine alkaloid alstonine was previously shown to have *in vitro* activity against *Plasmodium falciparum* malaria parasites and a slow-action activity that is different from other slow-action antiplasmodial compounds such as clindamycin.

Objectives: To investigate the action of the antiplasmodial compound alstonine by validating a putative resistance mutation and determining whether the activity of alstonine is linked to the mitochondrial electron transport chain.

Materials and methods: *In vitro* evolution of resistance was used to generate alstonine-resistant *P. falciparum*, followed by whole-genome sequencing and CRISPR/Cas9 gene editing of wildtype parasites to validate a putative resistance-associated mutation. Links to mitochondrial function were assessed using oxygen consumption rate measurements and activity of alstonine in *P. falciparum* expressing the yeast dihydroorotate dehydrogenase.

Results: *P. falciparum* parasites were selected with ~20-fold reduced sensitivity to alstonine compared to wild-type parasites. Whole-genome sequencing of alstonine-resistant *P. falciparum* sub-clones identified several mutations including a copy number variation and point mutation (A318P) in a gene encoding a putative inner-mitochondrial membrane protein (*Pf*MPV17). Introduction of the A318P mutation into the *Pf*MPV17 gene in wild-type *P. falciparum* yielded parasites with reduced alstonine sensitivity. While a direct link between alstonine action and mitochondrial respiratory function was not found, a transgenic *P. falciparum* line resistant to the cytochrome bc_1 inhibitor atovaquone and pyrimidine synthesis inhibitor DSM265 had reduced sensitivity to alstonine.

Conclusions: These data demonstrate that *Pf*MPV17 is linked to alstonine resistance and suggest that alstonine action is linked to the mitochondria and/or pyrimidine biosynthesis pathways.

Introduction

Malaria is a leading cause of infectious disease morbidity and mortality, with an estimated 263 million clinical cases and 597 000 deaths attributed to this disease in 2023.[1] Past decades have seen advances in options for prevention and treatment of malaria, including combination drugs such as artemisinin combination therapies (ACTs) and more recently the introduction of two malaria vaccines for children in sub-Saharan Africa (RTS,S/AS01 and R21/Matrix-M).[1,2] However, these vaccines provide only ~30%–75% protection[3–5] and their ability to produce long-lasting protective immunity is not yet clear.[6] While drugs remain vital to the prevention and treatment of malaria, parasite resistance is compromising the efficacy of all current drugs, including ACTs.[7–15] Of concern, malaria morbidity rates have plateaued over recent years,[1] which means that efforts to achieve malaria eradication need to include the development of drugs with different modes of action to current options to overcome malaria parasite resistance.[1]

In previous work, we reported the antiplasmodial activity of the indoloquinolizidine alkaloid alstonine, and hypothesized that this compound may have a different mode of action to current malaria drugs[16] (Figure 1). Alstonine has an *in vitro P. falciparum* 50% growth inhibitory concentration (IC_{50}) of 0.18 μM, >1000-fold selectivity for parasites over human cells (IC_{50} > 200 μM against human Neonatal Foreskin Fibroblasts), and a slow-action phenotype (239-fold lower IC_{50} in 96 h assays versus 48 h assays).[16] The activity of alstonine cannot be rescued by isopentenyl pyrophosphate,[16] a metabolite of the essential apicoplast organelle in *P. falciparum*.[17] This indicates that alstonine has a different slow-action mechanism from inhibitors such as clindamycin that target the apicoplast.[18] While alstonine is unlikely to be developed as a drug lead due to challenges associated with synthesis and possible off-target effects,[19,20] this compound has potential for use as a chemical tool to identify a novel drug target in *Plasmodium* that may be able to be exploited for malaria drug discovery.

In this study, the action of alstonine was investigated by generating *P. falciparum* parasites with *in vitro* resistance to this compound followed by whole-genome sequencing to identify mutations in resistant versus wild-type parasites. A mutation identified in a gene encoding the putative inner-mitochondrial membrane protein *Pf*MPV17 was then edited in wild-type *P. falciparum* and the sensitivity of transgenic lines to alstonine determined. Further studies included investigating the impact of alstonine on parasite oxygen consumption to determine whether alstonine directly inhibits mitochondrial electron transport chain (mtETC) activity and assessing the activity of alstonine against a *Plasmodium* mtETC inhibitor-resistant transgenic line.

Materials and methods

Compounds

Alstonine was supplied as a pure compound originally derived from NatureBank[21] housed at Griffith University, Australia. Chloroquine, clindamycin, atovaquone, pyrimethamine and artesunate were purchased from Sigma-Aldrich®, USA. Cycloguanil hydrochloride was purchased from Santa Cruz Biotechnology Inc, USA. Proguanil was supplied by Dr Andrew Riches, CSIRO, Melbourne, Australia. DSM265 was supplied by Professor Margaret Philips, UT Southwestern, TX, USA, and KAE609 supplied by Professor Kiaran Kirk, ANU, Canberra, Australia.

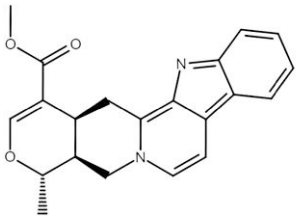

Figure 1. Structure, antiplasmodial activity and selectivity of alstonine. Data from.[16]

P. falciparum in vitro *growth inhibition assays*

P. falciparum infected erythrocytes were cultured in O^+ human erythrocytes (Australian Red Cross Lifeblood) in RPMI 1640 media (Gibco, USA) containing 10% heat-inactivated pooled human sera, 5 μg/mL gentamicin (Sigma, USA) and 50 μg/mL hypoxanthine (Sigma, USA). Cultures were maintained at 37°C in 5% O_2, 5% CO_2 and 90% N_2, essentially as described previously.[22] The activity of compounds was tested against *P. falciparum* using 72 h [^{3}H]-hypoxanthine incorporation assays, as previously described.[23] Briefly, serial dilutions of test compounds were added to 96-well plates (3596 Corning®), with the antimalarial drug chloroquine serving as a positive control. Synchronous ring-stage *P. falciparum* infected erythrocytes, prepared by sorbitol synchronization,[24] were added to each well at 0.25% parasitemia and 2.5% final haematocrit. After 48 h incubation, 0.25 μCi [^{3}H]-hypoxanthine (PerkinElmer®, USA) was added to each well and plates were incubated for a further 24 h and assay stopped by freezing the plates at −80°C. Cells were harvested onto Glass Microfibre mats (Filtech, USA) and tritium incorporation determined using a 1450 MicroBeta liquid scintillation counter (PerkinElmer®, USA). Percentage growth inhibition of compound treated versus vehicle only controls (0.5% DMSO) was determined and IC_{50} values calculated using nonlinear regression in GraphPad Prism®. Significant differences between IC_{50} values were determined using an unpaired *t*-test in GraphPad Prism®.

In vitro *evolution of* P. falciparum *resistance to alstonine*

P. falciparum 3D7 clone C3 (3D7-C3)[25] infected erythrocytes (1×10^7) were cultured with alstonine at 0.2 μM (alstonine IC_{50} = 0.18 ± 0.08 μM)[16] and parasite growth monitored every 1–3 days via microscopic examination of Quickdip (POCD, Australia) stained blood films. A starting concentration of ~$1\times IC_{50}$ was selected as this is routinely used for *P. falciparum* resistance selection studies.[26] When alstonine treated parasites were observed to be replicating at a similar rate to the untreated controls, compound pressure was gradually increased in a stepwise manner[26] for ~6 months until the parasites were surviving in >$10\times IC_{50}$ concentrations. The selected and wild-type clones were assessed using *in vitro* growth inhibition assays to determine sensitivity to alstonine and the control drug chloroquine (as described before). Once a resistance phenotype was confirmed for the 3D7-C3 selection, sub-cloning was performed via limiting dilution[27] and sensitivity to alstonine re-confirmed for three sub-clones.

Genome sequencing

Genomic DNA was isolated from *P. falciparum* infected erythrocytes using a DNeasy Blood and Tissue kit (Qiagen, USA). The Nextera XT kit (Illumina) was used to prepare DNA libraries from samples for whole-genome sequencing using the dual index protocol. The libraries were run on the

Illumina HiSeq 2500 in the Rapid Run mode with 100 bp paired-end reads and reads were aligned to the *Pf*3D7 reference genome (PlasmoDB)[28] as described previously.[29] Single-nucleotide polymorphisms (SNPs) and insertions and deletions (INDELs) were called with the Genome Analysis Toolkit's (GATK) HaplotypeCaller.[30,31] Variants were filtered by quality scores and sequencing bias statistics based on GATK's default filtering parameters. SNPs were filtered out if they met any of the following criteria: quality depth (QD) < 2.0, mapping quality (MQ) < 50.0, Phred-scaled *P* value using Fisher's exact test to detect strand bias (FS) > 60.0, symmetric odds ratio (SOR) > 4.0, *Z*-score from Wilcoxon rank sum test of alternative versus reference read mapping qualities (MQRankSum) < −12.5 and ReadPosRankSum (RPRS) < −8.0. INDELs were filtered out if they met any of the following criteria: QD < 2.0, RPRS < −20.0, FS > 200.0. Variants were annotated using snpeff (version 4.2).[32] Custom scripts were used to compare the variants between the parent sequence and the resistant clones. Variants that were present in both the parent and resistant clones, as well as those in genes that commonly mutate in culture but have no known role in drug resistance (i.e. *Pf*EMP1 gene family), were removed from consideration.

Determining DNA copy number by quantitative PCR

The genomic copy number (CN) of PF3D7_0502200 was estimated using quantitative PCR (qPCR) in an Applied Biosystems™ QuantStudio™ 6 Flex Real-Time PCR System (ThermoFisher, USA) using a SYBR green-based assay as previously described.[33] The housekeeping gene *Pf*seryl-tRNA synthetase was used as a reference. PCRs were performed in triplicate for two independent assays. Each reaction contained 1× reaction mix (FastStart Essential DNA Green Master; Life Science, Australia), 500 nM F1 and R2 primers (Table S6, available as Supplementary data at *JAC* Online) and 1 ng of DNA. Cycling was performed at 95°C for 10 min, followed by 35 cycles of 95°C for 30 s, 55°C for 30 s, then 60°C for 2 min. Cycle Threshold values were exported into Microsoft Excel and analysed with results presented as population mean CNs ± SEM.

Bioinformatic analysis

TMHMM[34] and Phobius[35] structural prediction tools were used to predict transmembrane domains and associated topology of *Pf*MPV17. AlphaFold 3 (Google DeepMind and EMBL-EBI)[36] was used to generate full 3D predicted models, with regions scored 0%–100% using a LDDT-Cα (local distance difference test; pLDDT).[37] The PyMol Molecular Graphics System (version 3.0, Schrödinger, LLC) was used to render and export the AlphaFold 3 models for publication.

CRISPR/Cas9 genome editing

CRISPR/Cas9 editing of the A318P (Gca/Cca) conferring point mutation and a silent control A318 silent (gcA/gcG) into *Pf*MPV17 was performed using the pDC2-coCas9-gRNA plasmid that possesses the hDHFR selection marker[38] (Figure S4). Two sgRNAs were designed using Benchling (www.benchling.com), and a donor template with 843-bp homology to the A318 target site was synthesized (ThermoFisher) and cloned into the *Aat*II-*Eco*RI sites of the pDC2-coCas9-gRNA plasmid using Gibson assembly. Plasmids were transfected by electroporation (310 kV, 950 µF) into *Pf*3D7 parasites, and selected with 2.5 nM WR99210 for 8 days. Editing of the recovered parasites was examined by Sanger sequencing of the bulk culture using PF3D7_0502200 F2 and R2 primers (Table S6), and clonal lines derived by limiting dilution.[27]

Seahorse oxygen consumption assay

Oxygen consumption rate (OCR) measurements of digitonin-permeabilized *Pf*3D7 parasites were performed as described previously.[39] Briefly, 200 mL of *Pf*3D7 culture at 4% haematocrit and at least 5% parasitemia was MACS® (Miltenyi Biotec) separated to obtain a trophozoite-dense sample, which was then saponin-lysed using 0.05% saponin at 37°C for 5 min. Isolated parasites were prepared at 5×10^7 parasites/mL in mannitol and sucrose-based (MAS) buffer supplemented with 10 mM malate and 0.002% digitonin. Isolated parasites were then seeded at 5×10^6 cells/well in a Cell-Tak-coated XFe96 cell culture plate (Agilent, USA) and centrifuged at 800×g, for 3 min at room temperature, to adhere the parasites to the bottom of the wells. Malate and digitonin supplemented MAS buffer (75 µL) was carefully added to the wells as to not disturb the cell monolayer. Analysis was performed using a Seahorse Bioscience XFe96 Extracellular Flux Analyzer as previously described.[39]

Results

Generation of P. falciparum *parasites resistant to alstonine*

A *Pf*3D7 clone (3D7-C3) was used to select for alstonine resistance using a stepwise selection method.[26] After ∼6 months of increasing alstonine exposure, parasites were able to grow in ∼20× alstonine IC_{50} (∼3 µM; termed 3D7-$C3^{ALST}$). A 32-fold higher IC_{50} was obtained for 3D7-$C3^{ALST}$ versus wild-type 3D7-C3 (IC_{50} 4.80 ± 0.49 and 0.15 ± 0.07 µM, respectively; $P<0.01$; Figure 2a; Table S1). By contrast, there was no significant difference in IC_{50} for the control drug chloroquine ($P>0.05$; Figure 2a; Table S1). Three independent 3D7-$C3^{ALST}$ sub-clones were generated via limiting dilution (termed 3D7-$C3^{ALST\text{-}E1}$, 3D7-$C3^{ALST\text{-}D7}$ and 3D7-$C3^{ALST\text{-}B1}$) and their alstonine resistance profiles confirmed (Figure 2b; Table S2). The alstonine IC_{50} of all sub-clones was 29–52-fold higher than for wild-type 3D7-C3 parasites ($P<0.05$) but there was no significant difference in IC_{50} values for the antimalarial drugs chloroquine, proguanil, atovaquone, clindamycin or the clinical candidate DSM265 (Figure 2b; Table S2; $P>0.05$).

Whole-genome sequencing identified mutations in the PfMPV17 gene in alstonine-resistant sub-clones

When comparing whole-genome sequencing data of 3D7-C3 wild-type parasites to the three 3D7-$C3^{ALST}$ sub-clones, a total of 12 genes with missense mutations were identified (Table S3). Of these, three were present in all three alstonine-resistant clones and are predicted to be in essential genes.[40] These genes encode the following predicted proteins: pre-mRNA-processing-splicing factor 8 (PF3D7_0405400), DNA topoisomerase 3 (PF3D7_1347100) and mitochondrial inner membrane protein MPV17 (*Pf*MPV17; PF3D7_0502200) (Table S3). Whole-genome sequencing also revealed a region within chromosome 5 (PF3D7_05_v3: 94808–12686) with a ∼3-fold increase in DNA CN for all three alstonine-resistant clones (Figure 3). This region includes 11 genes (Figure 3; Table S4), six of which are predicted to be essential, with a range of functions: putative vacuolar protein sorting-associated protein 11 VPS11 (PF3D7_0502000), HCNGP-like protein (PF3D7_0502100), conserved *Plasmodium* protein (PF3D7_0502500), Tim10/DDP family zinc finger protein (PF3D7_0502900), 50S ribosomal protein L28, apicoplast (PF3D7_0503000) and *Pf*MPV17 (PF3D7_0502200).

*Pf*MPV17 (PF3D7_0502200) was prioritized for further study as it is predicted to be essential in *Plasmodium*,[40,41] and all three alstonine-resistant sub-clones contained both a point mutation conferring an alanine to proline change (A318P) and a ∼3-fold *pfmpv17* CN increase. The *Pf*MPV17 A318P SNP was confirmed

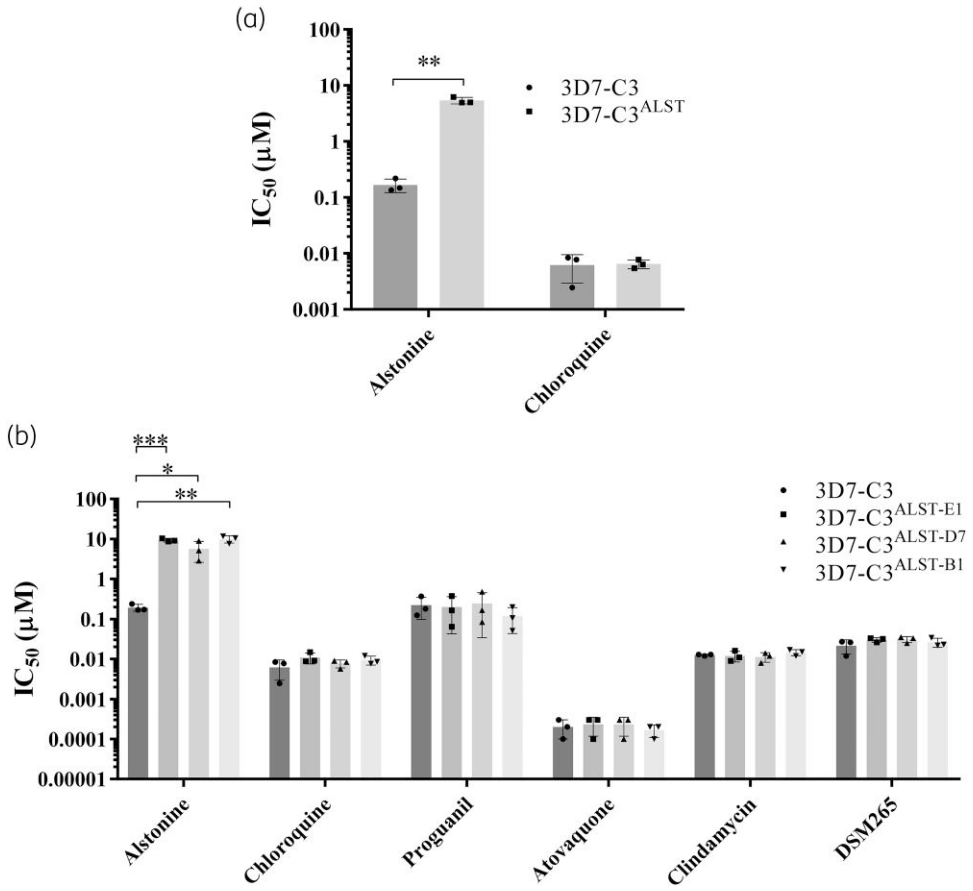

Figure 2. Alstonine-selected *P. falciparum* parasites and sub-clones are resistance to alstonine but remain sensitive to a panel of antiplasmodial compounds. (a) Sensitivity of wild-type clone 3D7-C3 versus the 3D7-C3^{ALST} population to alstonine and the control drug chloroquine. (b) Sensitivity of wild-type clone 3D7-C3 and alstonine-resistant sub-clones 3D7-C3$^{ALST-E1}$, 3D7-C3$^{ALST-D7}$ and 3D7-C3$^{ALST-B1}$ to alstonine and the antimalarial drugs chloroquine, proguanil, atovaquone, clindamycin and the antimalarial clinical candidate DSM265. In each case, the mean IC_{50} (±SD) is shown for three independent assays, each carried out in triplicate wells. A *P* value of >0.05 was considered not significant. * $P<0.05$, ** $P<0.01$, *** $P<0.001$.

via Sanger sequencing (Figure S1) and the genomic CN confirmed by qPCR (Figure 3). The *Pf*MPV17 gene is located on chromosome 5 of *P. falciparum*, with a 443 amino sequence encoding a protein of ~53 kDa.[28] *Pf*MPV17 has 24% amino acid similarity to its human homologue (UniProt P39210; data generated from Clustal Omega multiple sequence alignment, EMBL-EBI, UK; Figure S2) and has 100% amino acid identity across all *P. falciparum* lines deposited in the PlasmoDB genome database.[28] However, at the species level there is only ~50% amino acid identity between *P. falciparum* versus *P. malariae*, *P. vivax*, *P. knowlesi*, *P. ovale cutisi* or *P. ovale wallikeri*.[28] While there is limited information on MPV17 in other apicomplexans, *Toxoplasma*, *Cryptosporidium* and *Eimeria* have annotated *mpv17* genes[42] and the *T. gondii* MPV17 (gene ID: TGGT1_273290) is predicted to be fitness conferring.[43] *Pf*MPV17 transcription data[28] suggests expression in all asexual intraerythrocytic life stages, with highest expression at 24–32 h post-invasion.[44–47] Structure prediction tools TMHMM[34] and Phobius[35] were used to predict transmembrane topology and showed that *Pf*MPV17 is predicted to possess five transmembrane domains beginning on the inner-mitochondrial space (Figure 4a). A 3D AlphaFold 3[36] model predicted these transmembrane domains with high confidence, with pLDDT scores of >70 and >90, however, the long run of amino acids in the first half of the protein (amino acids 0–275) could not be predicted with confidence (pLDDT <50; Figure S3). The A318P mutation is located on the predicted matrix side of the second alpha helix, probably within the transmembrane domain (Figure 4a; Figure S3). It should be noted that the exact amino acid length of the predicted components of *Pf*MPV17 vary slightly between prediction tools, with the Phobius prediction represented in Figure 4a.

The PfMPV17 A318P mutation confers resistance to alstonine

To determine whether the A318P point mutation identified in alstonine-resistant clones mediates resistance to this compound, CRISPR/Cas9-based genome editing was used to introduce this mutation or a silent control mutation into wild-type *Pf*3D7 parasites (Figure S4). The A318P edited line (3D7-MPV17^{A318P}) demonstrated a 5-fold increase in IC_{50} compared to wild-type 3D7 parasites ($P<0.001$; Figure 4c; Table S5), confirming that

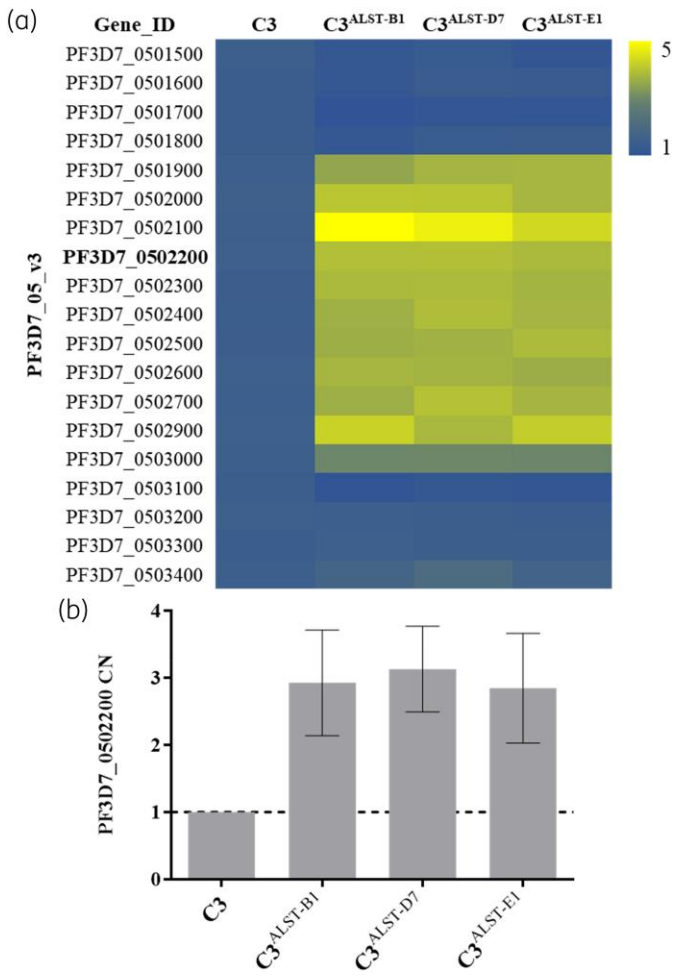

Figure 3. PF3D7_0502200 genomic CN increase in alstonine-resistant clones. (a) Heatmap of a region in chromosome 5 (PF3D7_05_v3: 94808–12686) identified in whole-genome sequencing to have a genomic CN increase in 3D7-C3^{ALST} clones. Data are shown as CN relative to the C3 parental clone, where yellow indicates an increase. The *Pf*MPV17 gene (PF3D7_0502200) is shown in bold. (b) The CN of PF3D7_0502200 was assessed in genomic DNA samples extracted from 3D7-C3^{ALST} clones and the parental clone 3D7-C3 by qPCR using an Applied Biosystems™ QuantStudio™ 6 Flex Real-Time PCR System (ThermoFisher, USA). Data are shown as mean CN (±SEM) relative to the C3 parental clone.

this mutation leads to alstonine resistance. There was no significant difference between the wild-type 3D7 line and the A318 silent control ($P>0.5$; Figure 4c; Table S5). Assessment of the activity of 3D7-MPV17^{A318P} parasites against a panel of antiplasmodial compounds compared to wild-type 3D7 parasites demonstrated that this line was not cross resistant to chloroquine, proguanil, atovaquone, DSM265, pyrimethamine, artesuante, KAE609 or cycloguanil ($P>0.05$; Figure 4c). Except for KAE609, the 3D7-MPV17^{silent} line displayed no significant change in IC_{50} values for all compounds tested in comparison to the wild-type parental line 3D7 ($P>0.05$; Figure 4c; Table S5). 3D7-MPV17^{silent} had a 2-fold decrease in IC_{50} for KAE609 versus wild-type 3D7 parasites, however, this was not highly significant ($P=0.049$).

Alstonine does not alter mitochondrial oxygen consumption rates in P. falciparum

To investigate an association between alstonine and the *Plasmodium* mtETC, the parasite mitochondrial OCR, a measure of mtETC activity, was determined using a Seahorse Bioscience XFe96 Extracellular Flux Analyzer.[39] As expected, injection of the mtETC inhibitors atovaquone and antimycin A resulted in a rapid decline of OCR (<5% 5 min post-baseline measurement; Figure 5). By contrast, injection of alstonine did not result in any appreciable decrease in OCR, maintaining >95% OCR at both 5 and 35 min post-baseline measurements, similar to the vehicle control (Figure 5).

Uncoupling P. falciparum *dihydroorotate dehydrogenase (DHODH) from the mtETC reduces alstonine activity*

Given that our data demonstrate that a mutation in the gene encoding the mitochondrial inner membrane protein *Pf*MPV17 confers resistance to alstonine, and a previous finding from our group that the atovaquone-resistant *P. falciparum* line C2B is 27-fold more sensitive to alstonine compared to atovaquone-sensitive 3D7 parasites[16] (the opposite effect to atovaquone to which C2B is highly resistant[23]), we compared the activity of alstonine against a *Pf*3D7 line expressing the ubiquinone-independent dihydroorotate dehydrogenase (class 1a DHODH) from *Saccharomyces cerevisiae* yeast (3D7-*y*DHODH).[48] In this line, DHODH is uncoupled from the electron transport chain, rendering this line resistant to mtETC inhibitors such as atovaquone[48,49] and *Pf*DHODH inhibitors such as DSM265.[50] As expected, 3D7-*y*DHODH parasites were resistant to atovaquone and DSM265 (Ri >290 and 709, respectively; Table 1). 3D7-*y*DHODH parasites were also resistant to alstonine with a 35-fold higher IC_{50} against 3D7-*y*DHODH versus 3D7 parasites ($P<0.05$; Table 1).

Discussion

Alstonine is an antiplasmodial compound with slow-action activity that differs from the slow 'delayed death' action of inhibitors such as clindamycin that target the apicoplast.[16] To further elucidate alstonine's antiplasmodial mode of action, alstonine-resistant clones were generated and shown to be >29-fold less sensitive to alstonine than the wild-type parental clone (Figure 2a). However, all alstonine-resistant clones remained sensitive to a panel of antiplasmodial compounds (Figure 2b), some of which target the mitochondria either directly or indirectly, suggesting that the activity of these antiplasmodial compounds is not affected by the mechanisms underlying resistance in the alstonine-resistant clones.

When the genomes of the alstonine-resistant clones were compared to that of the wild-type alstonine-sensitive parental clone, one gene with a common SNP and a 3-fold CNV in all three clones was identified. The gene (PF3D7_0502200) encodes the putative mitochondrial inner membrane protein *Pf*MPV17, which is involved in mitochondrial DNA maintenance in humans,[51–53] mice,[54,55] zebrafish,[56] *Drosophila*[57] and yeast.[58] Introduction of

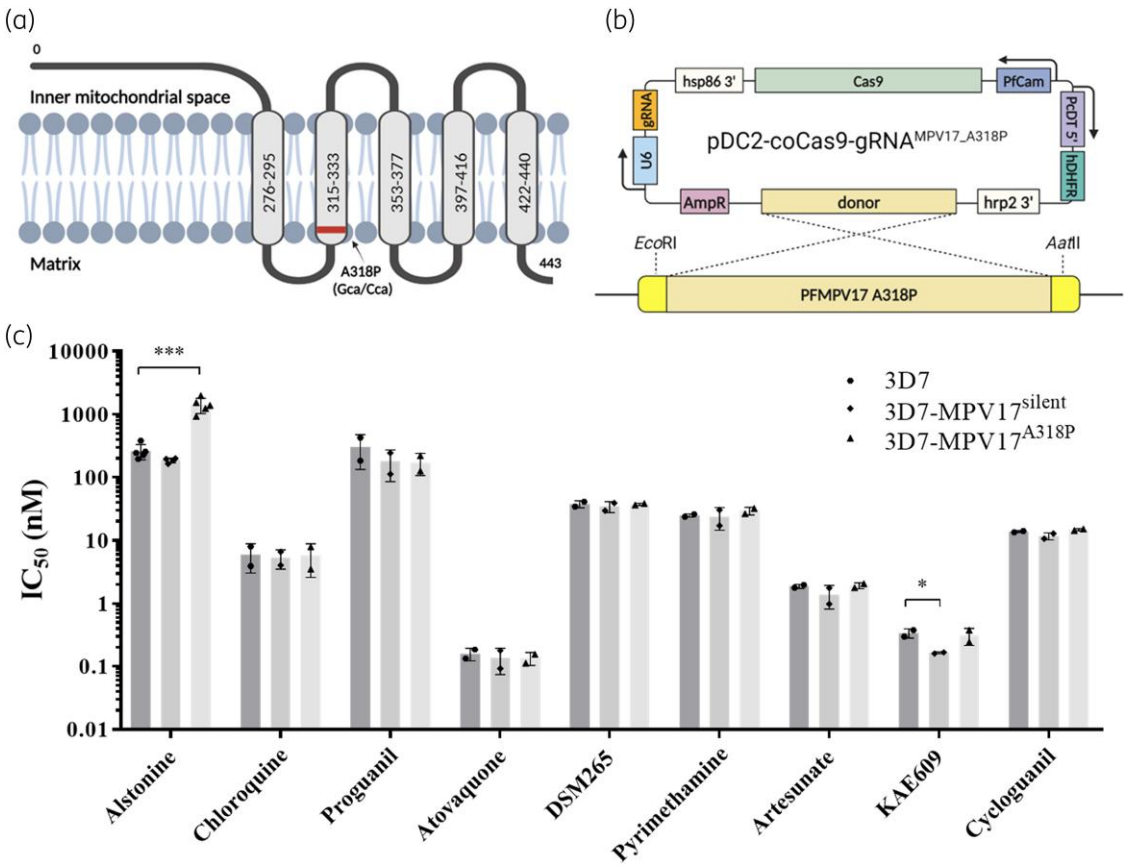

Figure 4. Predicted structure of *Pf*MPV17 and activity of alstonine and other antiplasmodial compounds against *P. falciparum Pf*MPV17 A318P transgenic parasites. (a) Predicted membrane topology of *Pf*MPV17 based on structural prediction software TMHMM (DTU Health Tech), Phobius (EMBL-EBI) and AlphaFold 3 (Google DeepMind and EMBL-EBI). There are five predicted transmembrane domains with amino acid lengths noted. Amino acid numbers shown are based on the Phobius prediction. Location of A318P mutation is highlighted in red on the predicted matrix side of the inner-mitochondrial membrane. (b) pDC2-coCas9-gRNA^{MPV17_A318P} plasmid used for genome editing of *P. falciparum* wild-type parasites to generate a silent and A318P mutation in *Pf*MPV17. (c) Activity of alstonine and other antiplasmodial compounds against wild-type 3D7, 3D7-MPV17^{silent} and 3D7-MPV17^{A318P}. Activity was determined using 72 h [^{3}H]-hypoxanthine incorporation growth inhibition assays. IC_{50} values were calculated using non-linear regression in GraphPad Prism® for at least two independent assays, each carried out in triplicate wells with data presented as mean values (±SD). *P* values were calculated using an unpaired *t*-test in GraphPad Prism®. A *P* value of >0.05 was considered not significant. * $P<0.05$, ** $P<0.01$, *** $P<0.001$.

the A318P mutation into *P. falciparum* resulted in an ~5-fold loss of sensitivity to alstonine but no change in sensitivity to a panel of antiplasmodial compounds (Figure 4c). While this provides evidence that the *Pf*MPV17 A318P mutation is associated with alstonine resistance, it should be noted that the clones derived from the alstonine-selected line were at least 6-fold more resistant to alstonine than the gene edited mutants. This suggests that other mutations are probably contributing to the high-level resistance phenotype in the alstonine-selected parasites. While additional studies would be needed to test this (e.g. overexpression of *Pf*MPV17 and phenotypic assessment), it is likely that the increased *Pf*MPV17 gene CN observed in the alstonine-selected clones contributes to the higher level of resistance in the selected versus gene edited clones. However, we cannot discount that the other mutations identified in these clones (Table S3 and S4) also play a role in alstonine resistance. For example, all three sub-clones had mutations in PF3D7_1347100, a topoisomerase gene (*pf*topo3) reported to interact with mitochondrial DNA (mtDNA) in schizont-stage *Plasmodium* parasites,[59] the developmental stage in which *Pf*MPV17 is highly expressed.[28] Interestingly, early studies proposed that alstonine, along with other β-carboline alkaloids, possess anticancer activity possibly linked to DNA damage and cell cycle arrest.[60–62]

In humans, functional loss of *Hs*MPV17 causes mitochondrial DNA depletion syndrome,[53] indicating a role for this protein in mtDNA maintenance. Under normal conditions, *Hs*MPV17 is a closed channel. However, in damaged mitochondria it is often open or leaky to preserve mitochondrial homeostasis.[54] Our structural predictions suggest that *Pf*MPV17 has five transmembrane domains and an estimated 265 amino acid N-terminal region that resides in the inner-mitochondrial membrane space (Figure 4a). If this is correct, the A318P *Pf*MPV17 mutation would reside between the matrix and the second transmembrane domain, and perhaps the change from alanine to proline, which is

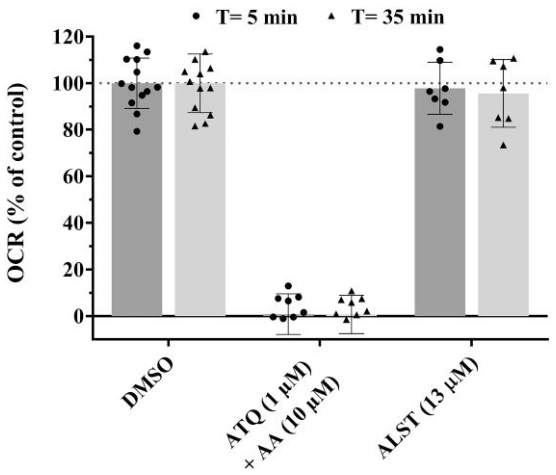

Figure 5. Alstonine does not inhibit mitochondrial respiration. *P. falciparum* schizonts were exposed to DMSO, atovaquone (ATQ, 1 μM) + antimycin A (AA, 10 μM) and alstonine (ALST, 13 μM) and OCR was measured at 5- and 35-min timepoints using a Seahorse Bioscience XFe96 Extracellular Flux Analyzer. Data represent mean OCR as a percentage of no treatment OCR ± SD of one assay from at least seven technical replicates ($n \geq 7$).

Table 1. Activity of alstonine against *P. falciparum* 3D7 and 3D7-yDHODH parasites

Compound	*Pf*3D7 line	*P. falciparum* IC_{50} (M)[a]	*P* value[b]	Ri[c]
Alstonine	3D7	$3.8\times10^{-7}\pm5.7\times10^{-8}$		
	*y*DHODH	$1.3\times10^{-5}\pm3.7\times10^{-6}$	0.001	35
Atovaquone	3D7	$2.1\times10^{-10}\pm9.3\times10^{-11}$		
	*y*DHODH	$>6.3\times10^{-8}$	—	>290
DSM265	3D7	$4.7\times10^{-8}\pm1.0\times10^{-8}$		
	*y*DHODH	$3.3\times10^{-5}\pm8.8\times10^{-6}$	0.006	709

Activity was determined using 72 h [^{3}H]-hypoxanthine incorporation growth inhibition assays.

[a]IC_{50} values were calculated using nonlinear regression in GraphPad Prism® for at least three independent assays, each carried out in triplicate wells with (±SD) shown. Where IC_{50} was not achieved, the highest concentration still giving >50% growth is shown.

[b]*P* values comparing 3D7 and 3D7-yDHODH IC_{50} were calculated using an unpaired *t*-test in GraphPad Prism®.

[c]Ri, resistance index; 3D7-*y*DHODH IC_{50}/3D7 IC_{50}.

a larger and less flexible amino acid,[63] interferes with alstonine binding or alternatively alters the conformational stability of the channel (Figure S3). While lowered levels of *Hs*MPV17 have been shown to impair mitochondrial respiration *in vitro*,[64] we did not observe alstonine-induced effects on mitochondrial oxygen consumption under the conditions examined (Figure 5). These preliminary data suggest that alstonine may not directly affect oxygen consumption in the parasite, however, given that the precise function of MPV17 in mitochondria has not been fully elucidated in humans and other species,[54] we cannot rule out the possibility that alstonine could be acting on other processes required for mtETC function.

To further explore a possible mitochondrial mode of action, atovaquone-resistant 3D7-*y*DHODH parasites were tested against alstonine. 3D7-*y*DHODH parasites use fumarate as an electron acceptor, uncoupling DHODH and pyrimidine biosynthesis from the mtETC in *P. falciparum* parasites.[48,49] Therefore, compounds that inhibit pyrimidine biosynthesis by targeting *Pf*DHODH (e.g. DSM265) or the mtETC (e.g. atovaquone) have reduced efficacy against 3D7-*y*DHODH compared to wild-type parasites.[48] In this study, 3D7-*y*DHODH were found to have a 35-fold reduced sensitivity to alstonine compared to 3D7 parasites (Table 1; $P=0.001$). While these data suggest that the action of alstonine is related to mitochondrial function and/or pyrimidine biosynthesis, the level of resistance was lower than for atovaquone and DSM265 which had a >290-fold and 709-fold reduced sensitivity for 3D7-*y*DHODH versus 3D7, respectively (Table 1), suggesting that a different mechanism is involved. This is further supported by the mutant MPV17 *P. falciparum* line (3D7-MPV17^{A318P}), which is resistant to alstonine, having an unchanged sensitivity (IC_{50}) to atovaquone and DSM265 (Table S5). Interestingly, in zebrafish, the loss of MPV17 has been linked to pyrimidine nucleotide metabolism through the impairment of DHODH activity[56] and bioinformatics analysis has shown that MPV17 and the trifunctional carbamoylphosphate synthetase 2, aspartate transcarbamylase and dihydroorotase, a cytosolic enzyme involved in pyrimidine production, are highly co-regulated.[56]

In conclusion, this study validated the A318P *Pf*MPV17 mutation as a mediator of alstonine resistance and suggests alstonine's mode of action is linked to the mitochondrial and/or pyrimidine synthesis pathways.

Acknowledgements

We thank the Australian Red Cross Lifeblood for the provision of human blood and sera for culture of *Plasmodium* parasites. *P. falciparum* 3D7 parasites overexpressing the yeast DHODH gene (3D7-*y*DHODH) were kindly provided by Dr Ben Dickerman, Burnet Institute, Melbourne Australia.

Funding

This work was supported by a Griffith University Postgraduate Research Scholarship and an Australian Government Research Training Program Stipend Scholarship to J.M.; a Griffith University GRIDD ECR grant to G.M.; a Ruth L. Kirschstein Institutional National Research Award from the National Institute of General Medical Sciences (T32 GM008666MRL to M.R.L.); National Institutes of Health and Bill & Melinda Gates Foundation Grants (1R01AI152533 and INV-039628 to E.W.); an Ideas grant from the National Health and Medical Research Council (GNT1182369 to A.G.M. and G.v.D.).

Transparency declarations

None to declare.

Data availability

Raw sequencing data for alstonine-selected parasite samples were deposited in the Sequence Read Archive (www.ncbi.nlm.nih.gov/sra) under BioProject accession PRJNA1157904.

Supplementary data

Figures S1 to S4 and Tables S1 to S6 are available as Supplementary data at *JAC* Online.

References

1 WHO. World Malaria Report, 2024. https://www.who.int/teams/global-malaria-programme/reports/world-malaria-report-2024.

2 Naddaf M. Second malaria vaccine to win global approval is cheaper and easier to make. *Nature* 2023; https://doi.org/10.1038/d41586-023-03115-1.

3 Abdulla S, Salim N, Machera F *et al.* Randomized, controlled trial of the long term safety, immunogenicity and efficacy of RTS,S/AS02(D) malaria vaccine in infants living in a malaria-endemic region. *Malar J* 2013; **12**: 11. https://doi.org/10.1186/1475-2875-12-11

4 RTS,S Clinical Trials Partnership; Agnandji ST, Lell B *et al.* First results of phase 3 trial of RTS,S/AS01 malaria vaccine in African children. *N Engl J Med* 2011; **365**: 1863–75. https://doi.org/10.1056/NEJMoa1102287.

5 Datoo MS, Dicko A, Tinto H *et al.* Safety and efficacy of malaria vaccine candidate R21/matrix-M in African children: a multicentre, double-blind, randomised, phase 3 trial. *Lancet* 2024; **403**: 533–44. https://doi.org/10.1016/S0140-6736(23)02511-4

6 Stanisic DI, Good MF. Malaria vaccines: progress to date. *BioDrugs* 2023; **37**: 737–56. https://doi.org/10.1007/s40259-023-00623-4

7 Ashley EA, Dhorda M, Fairhurst RM *et al.* Spread of artemisinin resistance in *Plasmodium falciparum* malaria. *N Engl J Med* 2014; **371**: 411–23. https://doi.org/10.1056/NEJMoa1314981

8 Balikagala B, Fukuda N, Ikeda M *et al.* Evidence of artemisinin-resistant malaria in Africa. *N Engl J Med* 2021; **385**: 1163–71. https://doi.org/10.1056/NEJMoa2101746

9 Fairhurst RM, Dondorp AM. Artemisinin-resistant *Plasmodium falciparum* malaria. *Microbiol Spectr* 2016; **4**. https://doi.org/10.1128/microbiolspec.EI10-0013-2016

10 Hamilton A, Haghpanah F, Hasso-Agopsowicz M *et al.* Modeling of malaria vaccine effectiveness on disease burden and drug resistance in 42 African countries. *Commun Med* 2023; **3**: 144. https://doi.org/10.1038/s43856-023-00373-y

11 Kagoro FM, Barnes KI, Marsh K *et al.* Mapping genetic markers of artemisinin resistance in *Plasmodium falciparum* malaria in Asia: a systematic review and spatiotemporal analysis. *Lancet Microbe* 2022; **3**: e184–92. https://doi.org/10.1016/S2666-5247(21)00249-4

12 Noedl H, Se Y, Schaecher K *et al.* Evidence of artemisinin-resistant malaria in western Cambodia. *N Engl J Med* 2008; **359**: 2619–20. https://doi.org/10.1056/NEJMc0805011

13 Uwimana A, Legrand E, Stokes BH *et al.* Emergence and clonal expansion of in vitro artemisinin-resistant *Plasmodium falciparum* kelch13 R561H mutant parasites in Rwanda. *Nat Med* 2020; **26**: 1602–8. https://doi.org/10.1038/s41591-020-1005-2

14 van Loon W, Oliveira R, Bergmann C *et al.* In vitro confirmation of artemisinin resistance in *Plasmodium falciparum* from patient isolates, Southern Rwanda, 2019. *Emerg Infect Dis* 2022; **28**: 852–5. https://doi.org/10.3201/eid2804.212269

15 Rosenthal PJ, Asua V, Bailey JA *et al.* The emergence of artemisinin partial resistance in Africa: how do we respond? *Lancet Infect Dis* 2024; **24**: e591–600. https://doi.org/10.1016/S1473-3099(24)00141-5

16 Arnold MSJ, Macdonald JR, Quinn RJ *et al.* Antiplasmodial activity of the natural product compounds alstonine and himbeline. *Int J Parasitol Drugs Drug Resist* 2021; **16**: 17–22. https://doi.org/10.1016/j.ijpddr.2021.04.003

17 Yeh E, DeRisi JL. Chemical rescue of malaria parasites lacking an apicoplast defines organelle function in blood-stage *Plasmodium falciparum*. *PLoS Biol* 2011; **9**: e1001138. https://doi.org/10.1371/journal.pbio.1001138

18 Ramya TN, Mishra S, Karmodiya K *et al.* Inhibitors of nonhousekeeping functions of the apicoplast defy delayed death in *Plasmodium falciparum*. *Antimicrob Agents Chemother* 2007; **51**: 307–16. https://doi.org/10.1128/AAC.00808-06

19 Linck VM, Bessa MM, Herrmann AP *et al.* 5-HT2A/C receptors mediate the antipsychotic-like effects of alstonine. *Prog Neuropsychopharmacol Biol Psychiatry* 2012; **36**: 29–33. https://doi.org/10.1016/j.pnpbp.2011.08.022

20 Linck VM, Herrmann AP, Piato AL *et al.* Alstonine as an antipsychotic: effects on brain amines and metabolic changes. *Evid Based Complement Alternat Med* 2011; **2011**: 418597. https://doi.org/10.1093/ecam/nep002

21 Camp D, Newman S, Pham NB *et al.* Nature bank and the Queensland Compound Library: unique international resources at the Eskitis Institute for Drug Discovery. *Comb Chem High Throughput Screen* 2014; **17**: 201–9. https://doi.org/10.2174/1386207317666140109120515

22 Trager W, Jensen JB. Human malaria parasites in continuous culture. *Science* 1976; **193**: 673–5. https://doi.org/10.1126/science.781840

23 Skinner-Adams TS, Fisher GM, Riches AG *et al.* Cyclization-blocked proguanil as a strategy to improve the antimalarial activity of atovaquone. *Commun Biol* 2019; **2**: 166. https://doi.org/10.1038/s42003-019-0397-3

24 Lambros C, Vanderberg JP. Synchronization of *Plasmodium falciparum* erythrocytic stages in culture. *J Parasitol* 1979; **65**: 418–20. https://doi.org/10.2307/3280287

25 Fisher GM, Cobbold SA, Jezewski A *et al.* The key glycolytic enzyme phosphofructokinase is involved in resistance to antiplasmodial glycosides. *mBio* 2020; **11**:e02842-20. https://doi.org/10.1128/mBio.02842-20

26 Luth MR, Gupta P, Ottilie S *et al.* Using in vitro evolution and whole genome analysis to discover next generation targets for antimalarial drug discovery. *ACS Infect Dis* 2018; **4**: 301–14. https://doi.org/10.1021/acsinfecdis.7b00276

27 Rosario V. Cloning of naturally occurring mixed infections of malaria parasites. *Science* 1981; **212**: 1037–8. https://doi.org/10.1126/science.7015505

28 Aurrecoechea C, Brestelli J, Brunk BP *et al.* PlasmoDB: a functional genomic database for malaria parasites. *Nucleic Acids Res* 2009; **37**: D539–43. https://doi.org/10.1093/nar/gkn814

29 Manary MJ, Singhakul SS, Flannery EL *et al.* Identification of pathogen genomic variants through an integrated pipeline. *BMC Bioinformatics* 2014; **15**: 63. https://doi.org/10.1186/1471-2105-15-63

30 McKenna A, Hanna M, Banks E *et al.* The genome analysis toolkit: a mapreduce framework for analyzing next-generation DNA sequencing data. *Genome Res* 2010; **20**: 1297–303. https://doi.org/10.1101/gr.107524.110

31 DePristo MA, Banks E, Poplin R *et al.* A framework for variation discovery and genotyping using next-generation DNA sequencing data. *Nat Genet* 2011; **43**: 491–8. https://doi.org/10.1038/ng.806

32 Cingolani P, Platts A, Wang le L *et al.* A program for annotating and predicting the effects of single nucleotide polymorphisms, SnpEff: SNPs in the genome of *Drosophila melanogaster* strain w1118; iso-2; iso-3. *Fly (Austin)* 2012; **6**: 80–92. https://doi.org/10.4161/fly.19695

33 Chavchich M, Gerena L, Peters J *et al.* Role of pfmdr1 amplification and expression in induction of resistance to artemisinin derivatives in *Plasmodium falciparum*. *Antimicrob Agents Chemother* 2010; **54**: 2455–64. https://doi.org/10.1128/AAC.00947-09

34 Möller S, Croning MD, Apweiler R. Evaluation of methods for the prediction of membrane spanning regions. *Bioinformatics* 2001; **17**: 646–53. https://doi.org/10.1093/bioinformatics/17.7.646

35 Käll L, Krogh A, Sonnhammer EL. A combined transmembrane topology and signal peptide prediction method. *J Mol Biol* 2004; **338**: 1027–36. https://doi.org/10.1016/j.jmb.2004.03.016

36 Abramson J, Adler J, Dunger J *et al*. Accurate structure prediction of biomolecular interactions with AlphaFold 3. *Nature* 2024; **630**: 493–500. https://doi.org/10.1038/s41586-024-07487-w

37 Mariani V, Biasini M, Barbato A *et al*. lDDT: a local superposition-free score for comparing protein structures and models using distance difference tests. *Bioinformatics* 2013; **29**: 2722–8. https://doi.org/10.1093/bioinformatics/btt473

38 Adjalley S, Lee MCS. CRISPR/Cas9 editing of the *Plasmodium falciparum* genome. *Methods Mol Biol* 2022; **2470**: 221–39. https://doi.org/10.1007/978-1-0716-2189-9_17

39 Ramesh S, Cihalova D, Rajendran E *et al*. Analysis of *Plasmodium falciparum* mitochondrial electron transport chain activity using seahorse XFe96 extracellular flux assays. *Bio Protoc* 2023; **13**: e4863. https://doi.org/10.21769/BioProtoc.4863

40 Zhang M, Wang C, Otto TD *et al*. Uncovering the essential genes of the human malaria parasite *Plasmodium falciparum* by saturation mutagenesis. *Science* 2018; **360**:eaap7847. https://doi.org/10.1126/science.aap7847

41 Bushell E, Gomes AR, Sanderson T *et al*. Functional profiling of a plasmodium genome reveals an abundance of essential genes. *Cell* 2017; **170**: 260–72.e8. https://doi.org/10.1016/j.cell.2017.06.030

42 Alvarez-Jarreta J, Amos B, Aurrecoechea C *et al*. VEuPathDB: the eukaryotic pathogen, vector and host bioinformatics resource center in 2023. *Nucleic Acids Res* 2024; **52**: D808–16. https://doi.org/10.1093/nar/gkad1003

43 Sidik SM, Huet D, Ganesan SM *et al*. A genome-wide CRISPR screen in toxoplasma identifies essential apicomplexan genes. *Cell* 2016; **166**: 1423–35.e12. https://doi.org/10.1016/j.cell.2016.08.019

44 Toenhake CG, Fraschka SA, Vijayabaskar MS *et al*. Chromatin accessibility-based characterization of the gene regulatory network underlying *Plasmodium falciparum* blood-stage development. *Cell Host Microbe* 2018; **23**: 557–69.e9. https://doi.org/10.1016/j.chom.2018.03.007

45 Otto TD, Wilinski D, Assefa S *et al*. New insights into the blood-stage transcriptome of *Plasmodium falciparum* using RNA-Seq. *Mol Microbiol* 2010; **76**: 12–24. https://doi.org/10.1111/j.1365-2958.2009.07026.x

46 Bártfai R, Hoeijmakers WA, Salcedo-Amaya AM *et al*. H2a.Z demarcates intergenic regions of the *Plasmodium falciparum* epigenome that are dynamically marked by H3K9ac and H3K4me3. *PLoS Pathog* 2010; **6**: e1001223. https://doi.org/10.1371/journal.ppat.1001223

47 Chappell L, Ross P, Orchard L *et al*. Refining the transcriptome of the human malaria parasite *Plasmodium falciparum* using amplification-free RNA-seq. *BMC Genomics* 2020; **21**: 395. https://doi.org/10.1186/s12864-020-06787-5

48 Dickerman BK, Elsworth B, Cobbold SA *et al*. Identification of inhibitors that dually target the new permeability pathway and dihydroorotate dehydrogenase in the blood stage of *Plasmodium falciparum*. *Sci Rep* 2016; **6**: 37502. https://doi.org/10.1038/srep37502

49 Painter HJ, Morrisey JM, Mather MW *et al*. Specific role of mitochondrial electron transport in blood-stage *Plasmodium falciparum*. *Nature* 2007; **446**: 88–91. https://doi.org/10.1038/nature05572

50 Baldwin J, Michnoff CH, Malmquist NA *et al*. High-throughput screening for potent and selective inhibitors of *Plasmodium falciparum* dihydroorotate dehydrogenase. *J Biol Chem* 2005; **280**: 21847–53. https://doi.org/10.1074/jbc.M501100200

51 Alonzo JR, Venkataraman C, Field MS *et al*. The mitochondrial inner membrane protein MPV17 prevents uracil accumulation in mitochondrial DNA. *J Biol Chem* 2018; **293**: 20285–94. https://doi.org/10.1074/jbc.RA118.004788

52 Karadimas CL, Vu TH, Holve SA *et al*. Navajo neurohepatopathy is caused by a mutation in the MPV17 gene. *Am J Hum Genet* 2006; **79**: 544–8. https://doi.org/10.1086/506913

53 Spinazzola A, Viscomi C, Fernandez-Vizarra E *et al*. MPV17 encodes an inner mitochondrial membrane protein and is mutated in infantile hepatic mitochondrial DNA depletion. *Nat Genet* 2006; **38**: 570–5. https://doi.org/10.1038/ng1765

54 Antonenkov VD, Isomursu A, Mennerich D *et al*. The human mitochondrial DNA depletion syndrome gene MPV17 encodes a non-selective channel that modulates membrane potential. *J Biol Chem* 2015; **290**: 13840–61. https://doi.org/10.1074/jbc.M114.608083

55 Dalla Rosa I, Cámara Y, Durigon R *et al*. MPV17 loss causes deoxynucleotide insufficiency and slow DNA replication in mitochondria. *PLoS Genet* 2016; **12**: e1005779. https://doi.org/10.1371/journal.pgen.1005779

56 Martorano L, Peron M, Laquatra C *et al*. The zebrafish orthologue of the human hepatocerebral disease gene MPV17 plays pleiotropic roles in mitochondria. *Dis Model Mech* 2019; **12**: dmm037226. https://doi.org/10.1242/dmm.037226

57 Corrà S, Checchetto V, Brischigliaro M *et al*. Drosophila Mpv17 forms an ion channel and regulates energy metabolism. *iScience* 2023; **26**: 107955. https://doi.org/10.1016/j.isci.2023.107955

58 Dallabona C, Marsano RM, Arzuffi P *et al*. Sym1, the yeast ortholog of the MPV17 human disease protein, is a stress-induced bioenergetic and morphogenetic mitochondrial modulator. *Hum Mol Genet* 2010; **19**: 1098–107. https://doi.org/10.1093/hmg/ddp581

59 Bansod S, Bung N, Singh P *et al*. Elucidation of an essential function of the unique charged domain of *Plasmodium topoisomerase* III. *Biochem J* 2020; **477**: 4745–67. https://doi.org/10.1042/BCJ20200318

60 Ahmad I, Fakhri S, Khan H *et al*. Targeting cell cycle by β-carboline alkaloids in vitro: novel therapeutic prospects for the treatment of cancer. *Chem Biol Interact* 2020; **330**: 109229. https://doi.org/10.1016/j.cbi.2020.109229

61 Beljanski M, Beljanski MS. Selective inhibition of in vitro synthesis of cancer DNA by alkaloids of beta-carboline class. *Exp Cell Biol* 1982; **50**: 79–87. https://doi.org/10.1159/000163131

62 Dassonneville L, Wattez N, Mahieu C *et al*. The plant alkaloid usambarensine intercalates into DNA and induces apoptosis in human HL60 leukemia cells. *Anticancer Res* 1999; **19**: 5245–50.

63 Morris AL, MacArthur MW, Hutchinson EG *et al*. Stereochemical quality of protein structure coordinates. *Proteins* 1992; **12**: 345–64. https://doi.org/10.1002/prot.340120407

64 Jacinto S, Guerreiro P, de Oliveira RM *et al*. MPV17 mutations are associated with a quiescent energetic metabolic profile. *Front Cell Neurosci* 2021; **15**: 641264. https://doi.org/10.3389/fncel.2021.641264